International Journal on Recent and Innovation Trends in Computing and Communication
ISSN: 2321-8169 Volume: 12 Issue: 2
Article Received: *25 November 2023* ***Revised:*** *12 December 2023* ***Accepted:*** *30 January 2024*

The Design and Assessment of Eudragit Gum Nanoparticles Containing Moronic Acid for Cancer Treatment

Deepshikha Verma[1], *Neeraj Sethi[2], Ashish Narain Dubey[3], Sushila Kaura[4], Yashika[5]
[1,3] Department of Chemistry, NIILM University, Kaithal
[2]Department of Biotechnology, OSGU, Hisar
[4]Department of Pharmacology, OSGU, Hisar
[5]Department of Chemistry, Postgraduate Govt College

***Corresponding Author**
Dr. Neeraj Sethi
Assistant Professor, Dept. of Biotechnology, OSGU, Hisar

Abstract: The employment of therapeutic techniques in the treatment of cancer is frequently associated with multidrug resistance or drug tolerance. The effectiveness of plant secondary metabolites in the fight against cancer can be significantly increased by synthesizing them at the nanometric scale. Moronic acid (MA) is one type of pentacyclic triterpenoid that inhibits the growth of cancer cells by blocking the regulation of cell growth. In this work, we used the oil-in-oil (O/O) emulsion solvent evaporation method to synthesize Eudragit nanoparticles (MENPs) loaded with MA. Enhancing the synergy and bioavailability of the nanoparticles was the aim of this intervention. The zeta potential of +28 mV observed in MENPs indicates the relative stability of the nanoformulations. MA was discovered to have 71.8% encapsulation efficiency. Transmission electron microscopy revealed that the MENPs' particle sizes ranged from 42 to 58 nm. The antioxidant and anticancer capabilities of the MENPs were significantly stronger and they showed a continuous release pattern when compared to the individual MA particles in their free state. The *in vitro* investigations showed that the combination of MA encapsulated in Eudragit had a greater inhibitory effect on the growth of A-549, MCF-7, and Hela cell lines as compared to the solo administration of MA. This finding confirms the potent anticancer properties of the encapsulated compounds.

Keywords: *Eudragit, Moronic acid, Anti-cancer, Nanoparticles*

Introduction

Oncology Nanotechnology is a swiftly growing field within the realm of medicine. Nanotechnology enables the creation of innovative nanoplatforms that are loaded with bioactive ingredients for combating cancer. Cytotoxic medicines and chemotherapy are commonly used together to treat several types of malignancies [1]. Nevertheless, there are adverse consequences associated with these traditional therapeutic methods, such as the development of drug resistance or tolerance [2, 3]. Currently, the utilization of nanotechnology in the development of remedies for severe ailments is more prevalent. Nanometric bioactive compounds exhibit heightened antioxidant and anticancer properties, together with exceptional absorption capabilities at small doses. The United States National Institute of Cancer has advocated for the investigation of the possible anticancer properties of many secondary metabolites present in plants [4,5]. Several phytochemicals, such as boswellic acid, moronic acid, and ursolic acid, have been demonstrated to possess cytotoxic properties [6]. Recent research has demonstrated that optimizing the physical characteristics of nanoparticles is crucial for achieving effective anti-cancer effects while minimizing adverse reactions [7]. The size, shape, and surface characteristics of nanoparticles affect their pharmacokinetic and pharmacodynamic properties.

Moronic acid (MA) is a pentacyclic triterpenoid that can be found in two forms: either as the aglycone of saponins or as a free carboxylic acid [8]. Glucocorticoids lead to a modification of glucocorticoid receptors, which leads to a reduction in Bcl2 (proteins that prevent cell death) in human

International Journal on Recent and Innovation Trends in Computing and Communication
ISSN: 2321-8169 Volume: 12 Issue: 2
Article Received: *25 November 2023* ***Revised:*** *12 December 2023* ***Accepted:*** *30 January 2024*

breast cancer cell lines (Michigan Cancer Foundation-7) [9, 10]. Methyl anthranilate (MA) is frequently included in pharmaceutical formulations for oral and topical delivery because of its minimal toxicity level [11]. The LD50 values for MA were determined to be 637 mg/kg (intraperitoneal treatment) and 8330 mg/kg (oral administration) in acute toxicity experiments done on mice [12].

When choosing an agent to encapsulate several drugs, it is crucial to consider the significant qualities of biodegradability and biocompatibility [13, 14]. Eudragit, a flexible group of synthetic polymers produced from methacrylic acid and acrylic acid esters, has garnered considerable interest in the realm of anticancer therapy. These polymers are extensively utilized in pharmaceutical formulations because of their exceptional biocompatibility, diversity in functional groups, and adjustable features such as solubility and release profiles. Eudragit polymers can be customized to alter the rates at which drugs are released, enhance drug stability, and specifically target certain locations in the body. This makes them highly valuable for developing sophisticated drug delivery systems for cancer therapy [15].

This work aimed to increase the bioavailability of moronic acid (MA) by using a polymeric nanoplatforms. This strategy was also intended to reduce adverse effects and achieve synergistic results. The inclusion of MA within the polymeric nanoparticles leads to a regulated and extended-release, resulting in improved therapeutic efficacy even at lower doses.

Experimental Details

Materials

The Eudragit was acquired from MP Biomedicals, LLC, a company based in France. The purchase of moronic acid was made from Sigma Aldrich, an Indian-based company. However, Minimum Essential Eagle Medium, Foetal bovine serum (FBS), penicillin, and streptomycin were acquired from Hi-media Laboratories Pvt. Ltd. in Mumbai, India. The cell lines employed in this work, namely A-549 (human lung adenocarcinoma epithelial cells), MCF-7 (human breast adenocarcinoma cells), and Hela (human cervical carcinoma cell line), were obtained from the National Centre for Cell Science (NCCS) in Pune. The chemicals utilized in the present investigation were of the analytical reagent grade.

Preparation of MA-loaded Eudragit nanoparticles (MENPs)

The production of the MENPs was achieved through the utilisation of the oil-in-oil emulsion solvent evaporation process. A solution was made by dissolving 150 mg of Eudragit and 100 mg of moronic acid in 100 ml of n-propanol. The designated solution was treated with 25 mg of Calcium stearate, and the resulting mixture was stirred magnetically at a speed of 1200 rpm for a period of 1 hour. The mixture was continuously stirred at a rate of 1200 revolutions per minute, maintained at a temperature of 42 degrees Celsius, for a period of 60 minutes. Afterwards, the mixture was divided by spinning it in a centrifuge at a rate of 8000 revolutions per minute, at a temperature of 4 degrees Celsius, for a period of 20 minutes. Once the pellet was gathered, it underwent freeze-drying while being held in suspension with cryoprotectant (D-Mannitol, 5% w/v).

Characterization of synthesized MENPs

To ascertain the mean size and size distribution (polydispersity index) of the optimized nanoformulations of MENPs, we employed a Zetasizer Nano ZS-90 manufactured by Malvern Instruments in Malvern, United Kingdom. The unbound drug was separated from the mixture by centrifuging the solution at 9000 revolutions per minute at a temperature of four degrees Celsius for a duration of thirty minutes. The resulting supernatant was then collected and evaluated using high-performance liquid chromatography (HPLC). The subsequent equation was employed to calculate the percentage of encapsulation efficiency:

The size and shape of the optimized batch of MENPs were examined using a transmission electron microscope (TEM-Hitachi-H-7501SSP/N-817-0520, Japan). The magnification factor was adjusted to 60,000, while the accelerating voltage was set to 80,000V. The TGA/DSC 3+ Star System, produced by Mettler Toledo AG, Analytical, Switzerland, is a device used for differential scanning calorimetry-thermogravimetric analysis.

In vitro release profile of MTDNPs

The release profile was examined using the dialysis sac approach. A total of 10 milligrams (mg) of MA, which had been enclosed in Eudragit nanoparticles, were placed within a dialysis sac. Subsequently, the sac was placed in a solution consisting of 10 ml of water, 25% ethanol, and 0.1 M phosphate buffer saline with a pH of 7.4. The solution was stirred vigorously at a constant temperature of 37 °C with a continuous swirling action at a rate of 100 revolutions per minute. A 1 ml sample was collected at regular time intervals of 1, 2, 3, 6, 12, and 24 hours and analyzed using High Performance Liquid Chromatography (HPLC) on an Agilent 1200 Infinity Series instrument. The analysis was performed using a ZORBAX SB C-18 column measuring 150 x 4.6 mm and having a particle size of 5 µm. The mobile phase used consisted of a blend of Acetonitrile and Water at a volumetric ratio of 80:20. The compounds of interest, MA, were detected at wavelengths of 210 nm, respectively, and had retention durations of 6.17 minutes.

International Journal on Recent and Innovation Trends in Computing and Communication
ISSN: 2321-8169 Volume: 12 Issue: 2
***Article Received:** 25 November 2023 **Revised:** 12 December 2023 **Accepted:** 30 January 2024*

Antioxidant activity

The DPPH assay was used to evaluate the antioxidant ability of MA and MENPs. The molecule 1,1-diphenyl-2-picrylhydrazyl (DPPH), a free radical, was fully dissolved in methanol at a concentration of 3.9 mg per 100 ml. The pure samples of MA, Eudragit, and MENPs were combined with DPPH and incubated in darkness for a duration of 30 minutes. This was performed three times to guarantee precision. The UV spectrophotometer was used to measure the absorbance of the combination at a wavelength of 517 nm to determine the level of DPPH inhibition. Eudragit nanoparticles were used as a negative control, whereas pure moronic acid was used as a positive control. The percentage inhibition of DPPH by pure MA, MENPs was calculated using the following formula:

Percent antioxidant activity = $\frac{\text{Absorbance of control} - \text{Absorbance of sample}}{\text{Absorbance of control}} \times 100$

In-vitro assay for cytotoxic activity (MTT assay)

Both normal and cancer cell lines were cultured in a medium containing inactivated fetal bovine serum (10%), streptomycin (100µl/ml), and penicillin (100µl/ml). The cells were subsequently placed in an incubator set at a temperature of 37°C and exposed to a carbon dioxide concentration of 5%. When the cells reached a point where they covered 75% of the surface, they were moved to a clean environment and further grown using a solution containing 0.25% trypsin. The chemicals and standards were prepared as stock solutions in DMSO with a concentration of micromoles per milliliter. Afterward, the medium was diluted at concentrations of 1µM, 10µM, 20µM, 50µM, and 100µM per ml. The cells were distributed in 96-well plates at a concentration of 5×103 cells per 100µl per well. The density of each cell line was evaluated according to their growth parameters. The wells were treated with different doses of MENPs (ranging from 0.1 to 1000µg/ml) and moronic acid for a duration of 3 days, with each treatment being performed in triplicate. This was done after an initial incubation period of 8 hours. After a three-day treatment period, the medium was replaced with 3µl of MTT solution (5mg/ml) and allowed to incubate for 3 hours. The percentage of cells displaying metabolic activity was assessed by comparing them to untreated control cells, using the conversion of 3-(4, 5-dimethylthiazol-2-yl) 2, 5 diphenyltetrazolium bromide (MTT) into Formazan crystals by mitochondria. The formazan crystals were dissolved in dimethyl sulfoxide (DMSO) and the absorbance was quantified at 570 nm using a microplate reader. The effectiveness of MENPs in treating cancer was evaluated using pure MA as a benchmark through the MTT test on three types of cells: A-549 (human lung adenocarcinoma epithelial cells), MCF-7 (human breast adenocarcinoma cells), and Hela (human cervical carcinoma cell line). The formula was used to determine the proportion of cell growth inhibition (1) and cytotoxicity (2).

%viability = $(A_{Tr} - A_{Bl}) / (A_{Ct} - A_{Bl}) \times 100$ ……. (1)

Where A_{Tr} = Absorbance for treated cells (drug); A_{Bl} = Absorbance for blank

A_{Ct} = Absorbance for control (untreated)

%cytotoxicity = 100 – Percent cell survival (%) ……. (2)

Results and Discussion

Particle Size and Zeta Potential

A comprehensive examination was performed on the MENPs to ascertain their particle size and zeta potential. The dimensions of the MENPs were identified as 148 nm (Fig 1), and the zeta potential was assessed as +23 mV (Fig 2), suggesting the considerable stability of the produced nanoformulations

Percent encapsulation efficiency

The effectiveness of encapsulation depends on the particular molecule, technique, encapsulating materials, and media employed in the synthesis of nanoparticles [22]. The encapsulation effectiveness percentage was measured by evaluating the supernatant using High-Performance Liquid Chromatography (HPLC) to quantify the quantity of unbound medicine. The results demonstrated that the encapsulation efficiency of MA was 72.5%, as depicted in Figure 5. Both Moronic acids have hydrophobic characteristics. They exhibit exceptional solubility in a eudragit solution prepared with n-propanol. Due to its hydrophobic nature, Eudragit showed a strong affinity towards both MA. Consequently, the drug was encapsulated more efficiently in Eudragit due to this affinity.

Morphological characterization of* MENPs *by TEM

The Magnetic Nanoparticles (MENPs) were isolated and exhibited a uniform spherical morphology, as evidenced by Transmission Electron Microscopy analysis (Fig 3). Their dimensions varied between 45 and 55 nanometers. The size of the nanoparticles was shown to fluctuate when measured using Particle Size Analyzer (PSA) and Transmission Electron Microscopy (TEM). The PSA method considers the fluidized ionic environment around the nanoparticles, whereas TEM analyzes the size of the particles in a dehydrated and isolated atmosphere, leading to a reduction in particle size. The size of nanoparticles has an impact on their rate of release [23, 24]. Nanoparticles are dispersed throughout different organs in the body according to their shape and size. The morphology and dimensions of nanoparticles are essential factors in regulating their durability, biocompatibility, and ability to permeate cellular tissues [25]. Nanoparticles with smaller dimensions have a

International Journal on Recent and Innovation Trends in Computing and Communication
ISSN: 2321-8169 Volume: 12 Issue: 2
Article Received: *25 November 2023* ***Revised:*** *12 December 2023* ***Accepted:*** *30 January 2024*

longer duration of retention in the bloodstream compared to nanoparticles with bigger dimensions [26].

FTIR Analysis of Drug Samples

FTIR spectroscopy is used for studying the interaction studies [27] and evaluating the nanoencapsulation of bioactive substances [28]. Figure 4 exhibits the FTIR spectra of the separate constituents: unadulterated medicine MA, Eudragit, and MENPs. The MA FTIR spectrum displays absorption peaks at 3234 cm-1, which correspond to the -OH group, and at 2897.0 cm-1 and 2244 cm-1 for the terminal –CH3 groups. The wavenumber values of 1345 cm-1 and 3453 cm-1 correspond to the stretching of -NH2. The FTIR spectrum of Eudragit, shown in Figure 4 C, displays a peak at 3346 cm-1, which corresponds to the stretching of –OH groups, and a peak at 2845 cm-1, indicating the stretching of aliphatic –CH groups in Eudragit. The FTIR spectra of MENPs, as shown in Figure 4D, display alterations at wave numbers of 3400 cm-1, 1434 cm-1, 2453 cm-1, and 2871 cm-1. This region corresponds to the range of infrared stretching vibrations shown by functional groups such as hydroxyl (-OH), double bond (C=C) stretching, methyl group (-CH3) stretching, and carbon-hydrogen (C-H) stretching. The drug molecule exhibits weak intermolecular forces, specifically dipole-dipole interactions, hydrogen bonding (with electronegative atoms like N, O, F), and weak Van der Waals forces (dependent on mass), with the OH groups in Eudragit. The drugs and inactive substances show identifiable peaks in the FTIR spectrum. The maximum intensity of the signal reduced and the positions of the bands moved, suggesting the occurrence of chemical interaction between moronic acid and Eudragit.

In-vitro drug release

The continuous release of bioactive chemicals from nanoparticles protects rapid metabolism and breakdown [29]. The in vitro drug release of MA and MENP is illustrated in Figure 6. The in-vitro drug release data demonstrates that 95% of the pure MA is released within a time frame of 4 hours. MENPs exhibit sustained drug release as a result of Eudragit emulsification. After one hour of treatment, Magnetic Nanoparticles (MENPs) release 20% of Methylamine (MA). Magnetic nanoparticles (MENPs) released 80% of the MA compound within 24 hours. Hydrophobic (nonpolar) maleic anhydride (MA) enables magnetic iron oxide nanoparticles (MENPs) to gradually release MA. Eudragit created a unified structure around MA, guaranteeing their extended distribution.

DSC Analysis

The differential scanning calorimetry (DSC) thermogram of free MA exhibits a less intense endothermic peak and advancing crests at 150˚C, which suggests the presence of the medication. The DSC thermograms of moronic acid reveal two distinct endothermic peaks. The initial endothermic peak observed at 286˚C, albeit it has a low strength, indicates the presence of moronic acid [30]. The sudden and strong climax verified its characteristic of being crystalline. The lack of prominent crests in all DSC graphs suggests that the nanoformulations are amorphous and that the medication is suitable for its amorphous state. Eudragit nanoparticles containing moronic acid display an endothermic peak with a low intensity of around 374˚C, showing their amorphous nature. The initial decomposition of the nanoparticles starts at 318˚C, while the secondary decomposition takes place at 445˚C. The presence of a low-intensity, blunt peak hump serves as evidence of its amorphous nature. In comparison to MENPs, the fake nanoformulations exhibit a relatively little increase in temperature throughout the process of liquefaction, as seen in Figure 7B. The peak of the melting point of Eudragit nanoparticles loaded with MA changed to a higher temperature, suggesting the production of a co-amorphous phase.

Thermo-gravimetric analytical studies

The highest weight reduction of the dummy Eudragit nanoformulations was observed at a temperature of 359˚C. The melting endotherm movement of MENPs was significantly greater than that of the dummy Eudragit nanoformulations, with the maximum weight loss occurring at 412˚C. The results suggest that the formation of the co-amorphous phase varied between the Eudragit nanoformulations containing MA and the dummy nanoformulations (Fig 7).

Anti-oxidant activity

The DPPH assay measures the level of antioxidant activity of encapsulated molecules [31]. DPPH, also known as 1,1-diphenyl-2-picrylhydrazyl, is a stable free radical that contains unpaired electrons spread evenly across its structure, resulting in a distinct deep violet hue. Absorption takes place at a wavelength of around 517 nm [32]. The violet color of DPPH solutions is uniformly lost when they are combined with molecules that donate hydrogen. MA is a widely recognized antioxidant. The process of incubating the antioxidant molecules MA with DPPH, which acts as a hydrogen atom donor, resulted in the formation of a stable, non-radical form of DPPH. This transformation caused the color of the DPPH to change from violet to pale yellow. Therefore, the absorption band diminished. MA block DPPH undergoes hydrogen atom release, causing the DPPH to become labile. Because of their extremely small size, the nanometric MENPs showed a greater ability to block DPPH

compared to MA alone during the period of dark incubation. This resulted in their protection from oxidation (Fig 8).

Anti-cancer activity

Nanoparticles exhibit cytotoxicity due to their extensive surface area, which enables efficient drug administration and potential for anticancer effects [33]. Nanoparticles of 100 nm in size can readily penetrate tumor cells by retention and vascular penetration [34]. The anticancer effects of NPs are size-dependent [35,40]. Microscopic nanoparticles exhibit enhanced tumor penetration capabilities. The enzyme mitochondrial dehydrogenase is present within live cells. The MTT dye is broken down, causing the pale-yellow tetrazolium ring structure to be disrupted. This results in the formation of dark purple formazan crystals, which then build up in cells [41-48]. The current study demonstrated that magnetic-engineered nanoparticles (MENPs) exhibited superior efficacy in inhibiting cancer growth compared to the pure active drug alone. In laboratory conditions, the use of Eudragit-encapsulated MA was found to be more effective in inhibiting the growth of A-549, MCF-7, and Hela cells compared to the unencapsulated medications. Table 1 displays the IC50 values (µg/ml) of the nanoparticles that were produced, as well as the reference medicines moronic acid. When compared to regular pharmaceuticals MA alone, MENPs had strong anticancer effects with IC50s of 4.1, 3.8, and 4.2 µg/ml against A-549, MCF-7, and Hela cell lines as observed through optical microscopy. The combined effect of MA in MENPs resulted in a potent anticancer effect.

Conclusions

Nanotechnology has greatly enhanced the process of formulating and developing treatments, hence enhancing the potential for efficiently treating and curing diseases. Advancements in nano-drug delivery technology have enabled oncology researchers to explore the synergistic effects of medications by utilizing nanoparticles with larger payloads, including dual drug delivery. Although numerous anticancer drugs have been created, the main obstacles to these treatments are drug tolerance/resistance, limited bioavailability, and short drug residence time. Novel nanoformulations containing more potent excipients can be utilized to improve solubility, bioavailability, therapeutic potential, and adverse effect profiles. According to the findings of this study, a novel formulation of Eudragit nanoparticles loaded with moronic acid has great potential in combating cancer. This is because it possesses both antioxidant and anticancer capabilities that work together beneficially.

Conflict of Interest

There is no conflict of interest whatever.

References

1. Thakral, S., Thakral, N. K., & Majumdar, D. K. (2013). Eudragit®: a technology evaluation. *Expert opinion on drug delivery*, *10*(1), 131-149.
2. Li, C. F., Li, Y. C., Chen, L. B., Wang, Y., & Sun, L. B. (2016). Doxorubicin-loaded Eudragit-coated chitosan nanoparticles in the treatment of colon cancers. *Journal of Nanoscience and Nanotechnology*, *16*(7), 6773-6780..
3. Thakral, N. K., Ray, A. R., & Majumdar, D. K. (2010). Eudragit S-100 entrapped chitosan microspheres of valdecoxib for colon cancer. *Journal of Materials Science: Materials in Medicine*, *21*, 2691-2699.
4. Sethi, N., Bhardwaj, P., Kumar, S., & Dilbaghi, N. (2019). Development and Evaluation of Ursolic Acid Co-Delivered Tamoxifen Loaded Dammar Gum Nanoparticles to Combat Cancer. *Advanced Science, Engineering and Medicine*, *11*(11), 1115-1124.
5. Sethi, N., Bhardwaj, P., Kumar, S., & Dilbaghi, N. (2019). Development And Evaluation Of Ursolic Acid Loaded Eudragit-E Nanocarrier For Cancer Therapy. *International Journal of Pharmaceutical Research (09752366)*, *11*(2).
6. Saini, A., Budania, L. S., Berwal, A., & Sethi, S. K. N. (2023). Screening of the Anticancer Potential of Lycopene-Loaded Nanoliposomes. *Tuijin Jishu/Journal of Propulsion Technology*, *44*(4), 1372-1383.
7. Xu, M., Han, X., Xiong, H., Gao, Y., Xu, B., Zhu, G., & Li, J. (2023). Cancer nanomedicine: emerging strategies and therapeutic potentials. *Molecules*, *28*(13), 5145.
8. Dhanda, P., Sura, S., Lathar, S., Shoekand, N., Partishtha, H., & Sethi, N. (2022). Traditional, phytochemical, and biological aspects of Indian spider plant.
9. Kaura, S., Parle, M., Insa, R., Yadav, B. S., & Sethi, N. (2022). Neuroprotective effect of goat milk. *Small Ruminant Research*, *214*, 106748.
10. Sood, A., Dev, A., Mohanbhai, S. J., Shrimali, N., Kapasiya, M., Kushwaha, A. C., ... & Karmakar, S. (2019). Disulfide-bridged chitosan-eudragit S-100 nanoparticles for colorectal cancer. *ACS Applied Nano Materials*, *2*(10), 6409-6417..
11. Kumar, R., Sethi, N., & Kaura, S. (2022). Bio-processing and analysis of mixed fruit wine manufactured using Aegle marmelos and Phoenix dactylifer.
12. Poonam, D., Sethi, N., Pal, M., Kaura, S., & Parle, M. (2014). Optimization of shoot multiplication media for micro propagation of Withania somnifera: an endangered

medicinal plant. *Journal of Pharmaceutical and Scientific Innovation (JPSI)*, *3*(4), 340-343.

13. Suman, J., Neeraj, S., Rahul, J., & Sushila, K. (2014). Microbial synthesis of silver nanoparticles by Actinotalea sp. MTCC 10637. *American Journal of Phytomedicine and Clinical Therapeutics*, *2*, 1016-23.
14. Chehelgerdi, M., Chehelgerdi, M., Allela, O. Q. B., Pecho, R. D. C., Jayasankar, N., Rao, D. P., & Akhavan-Sigari, R. (2023). Progressing nanotechnology to improve targeted cancer treatment: overcoming hurdles in its clinical implementation. Molecular cancer, 22(1), 169.
15. Milind, P., Sushila, K., & Neeraj, S. (2013). Understanding gout beyond doubt. *International Research Journal of Pharmacy*, *4*(9), 25-34.
16. Wang, G., Yang, Y., Yi, D., Yuan, L., Yin, P. H., Ke, X., ... & Tao, M. F. (2022). Eudragit S100 prepared pH-responsive liposomes-loaded betulinic acid against colorectal cancer in vitro and in vivo. *Journal of Liposome Research*, *32*(3), 250-264..
17. Sethi, N., Kaura, S., Dilbaghi, N., Parle, M., & Pal, M. (2014). Garlic: A pungent wonder from nature. *International research journal of pharmacy*, *5*(7), 523-529.
18. Verma, R., Bhatt, S., Dutt, R., Kumar, M., Kaushik, D., & Gautam, R. K. (2023). Establishing Nanotechnology-Based Drug Development for Triple-Negative Breast Cancer Treatment. Drug and Therapy Development for Triple Negative Breast Cancer, 153-180.
19. Milind, P., Renu, K., & Kaura, S. (2013). Non-behavioral models of psychosis. *International Research Journal of Pharmacy*, *4*(8), 89-95.
20. Kriplani, P., & Guarve, K. (2022). Eudragit, a nifty polymer for anticancer preparations: a patent review. *Recent Patents on Anti-Cancer Drug Discovery*, *17*(1), 92-101..
21. Kaura, S., & Parle, M. (2015). Anti-Alzheimer potential of green moong bean. *Int. J. Pharm. Sci. Rev. Res*, *37*(2), 178-182.
22. Li, H., Fu, Q., Muluh, T. A., Shinge, S. A. U., Fu, S., & Wu, J. (2023). The Application of Nanotechnology in Immunotherapy based Combinations for Cancer Treatment. Recent Patents on Anti-Cancer Drug Discovery, 18(1), 53-65.
23. Monga, S., Sethi, N., Kaura, S., Parle, M., & Lohan, S. (2014). Effect of 6-benzyl amino purine hormone on the shooting growth of Ocimum gratissimum. *L. International Research Journal of Pharmacy*, *5*(2), 106-108.
24. Sathe, A., Prajapati, B. G., & Bhattacharya, S. (2023). Understanding the charismatic potential of nanotechnology to treat skin carcinoma. Medical Oncology, 41(1), 22.
25. Milind, P., Bansal, N., & Kaura, S. (2014). Take soybean to remain evergreen. *International Research Journal of Pharmacy*, *5*(1), 1-6.
26. Gupta, A., Sood, A., Dhiman, A., Shrimali, N., Singhmar, R., Guchhait, P., & Agrawal, G. (2022). Redox responsive poly (allylamine)/eudragit S-100 nanoparticles for dual drug delivery in colorectal cancer. *Biomaterials Advances*, *143*, 213184..
27. Parle, M., Malik, J., & Kaura, S. (2013). Life style related health hazards. *Int. Res. J. Pharm*, *4*(11), 1-5.
28. Kumar, P., Mangla, B., Javed, S., Ahsan, W., Musyuni, P., Ahsan, A., & Aggarwal, G. (2023). Gefitinib: an updated review of its role in the cancer management, its nanotechnological interventions, recent patents and clinical trials. Recent Patents on Anti-Cancer Drug Discovery, 18(4), 448-469.
29. Patel, N. V., Sheth, N. R., & Mohddesi, B. (2015). Formulation and evaluation of genistein–a novel isoflavone loaded chitosan and eudragit® nanoparticles for cancer therapy. *Materials Today: Proceedings*, *2*(9), 4477-4482..
30. Parle, M., & Kaura, S. (2013). Green chilli: A memory booster from nature. *Ann. Pharm. and Pharm. Sci*, *4*(1), 17-21.
31. Kaura, S., & Parle, M. (2017). Evaluation of nootropic potential of green peas in mice. *Journal of Applied Pharmaceutical Science*, *7*(5), 166-173.
32. Yurtdaş-Kırımlıoğlu, G., Görgülü, Ş., & Berkman, M. S. (2020). Novel approaches to cancer therapy with ibuprofen-loaded Eudragit® RS 100 and/or octadecylamine-modified PLGA nanoparticles by assessment of their effects on apoptosis. *Drug Development and Industrial Pharmacy*, *46*(7), 1133-1149.
33. Kaura, S., & Parle, M. (2017). Anti-ageing activity of moong bean sprouts. *International Journal of Pharmaceutical Sciences and Research*, *8*(10), 4318-4324.
34. Zheng, N., Yao, Z., Tao, S., Almadhor, A., Alqahtani, M. S., Ghoniem, R. M., ... & Li, S. (2023). Application of nanotechnology in breast cancer screening under obstetrics and gynecology through the use of CNN and ANFIS. Environmental Research, 234, 116414.
35. Meenakshi, P., Neeraj, S., Sushila, K., & Milind, P. (2014). Plant regeneration studies in Safed musli (Chlorophytum sp.). *Int J Res Ayuveda Pharm*, *5*, 195-98.
36. Zhang, P., Xiao, Y., Sun, X., Lin, X., Koo, S., Yaremenko, A. V., ... & Tao, W. (2023). Cancer

nanomedicine toward clinical translation: Obstacles, opportunities, and future prospects. Med, 4(3), 147-167.

37. Ahmed, O. A., Badr-Eldin, S. M., Caruso, G., Fahmy, U. A., Alharbi, W. S., Almehmady, A. M., & Mady, F. M. (2022). Colon Targeted Eudragit Coated Beads Loaded with Optimized Fluvastatin-Scorpion Venom Conjugate as a Potential Approach for Colon Cancer Therapy: In Vitro Anticancer Activity and In Vivo Colon Imaging. *Journal of Pharmaceutical Sciences*, *111*(12), 3304-3317.
38. Kumari, A., Yadav, S. K., Pakade, Y. B., Singh, B., & Yadav, S. C. (2010). Development of biodegradable nanoparticles for delivery of quercetin. *Colloids and Surfaces B: Biointerfaces*, *80*(2), pp.184-192.
39. Khuroo, T., Verma, D., Talegaonkar, S., Padhi, S., Panda, A.K. and Iqbal, Z., 2014. Topotecan–tamoxifen duple PLGA polymeric nanoparticles: investigation of in vitro, in vivo and cellular uptake potential. *International journal of pharmaceutics*, *473*(1-2), pp.384-394.
40. Song, J., Wang, Y., Song, Y., Chan, H., Bi, C., Yang, X., Yan, R., Wang, Y. and Zheng, Y., 2014. Development and characterisation of ursolic acid nanocrystals without stabiliser having improved dissolution rate and in vitro anticancer activity. *Aaps Pharmscitech*, *15*(1), pp.11-19.
41. Molyneux, P., 2004. The use of the stable free radical diphenylpicrylhydrazyl (DPPH) for estimating antioxidant activity. *Songklanakarin J. Sci. Technol*, *26*(2), pp.211-219.
42. Dahiya, S., Rani, R., Kumar, S., Dhingra, D. and Dilbaghi, N., 2017. Chitosan-gellan gum bipolymeric nanohydrogels—a potential nanocarrier for the delivery of epigallocatechin gallate. *BioNanoScience*, *7*(3), pp.508-520.
43. Subudhi, M. B., Jain, A., Jain, A., Hurkat, P., Shilpi, S., Gulbake, A., & Jain, S. K. (2015). Eudragit S100 coated citrus pectin nanoparticles for colon targeting of 5-fluorouracil. *Materials*, *8*(3), 832-849.
44. Siegler, E.L., Kim, Y.J. and Wang, P., 2016. Nanomedicine targeting the tumor microenvironment: Therapeutic strategies to inhibit angiogenesis, remodel matrix, and modulate immune responses. *Journal of Cellular Immunotherapy*, *2*(2), pp.69-78.
45. Piktel, E., Niemirowicz, K., Wątek, M., Wollny, T., Deptuła, P. and Bucki, R., 2016. Recent insights in nanotechnology-based drugs and formulations designed for effective anti-cancer therapy. *Journal of nanobiotechnology*, *14*(1), pp.39-53.
46. Saraf, A., Dubey, N., Dubey, N., & Sharma, M. (2019). Box Behnken design based development of curcumin loaded Eudragit S100 nanoparticles for site-spcific delivery in colon cancer. *Research Journal of Pharmacy and Technology*, *12*(8), 3672-3678..
47. Gerlier, D. and Thomasset, N., 1986. Use of MTT colorimetric assay to measure cell activation. *Journal of immunological methods*, *94*(1-2), pp.57-63.
48. Saraf, A., Dubey, N., Dubey, N., & Sharma, M. (2019). Box Behnken design-based development of curcumin loaded Eudragit S100 nanoparticles for site-spcific delivery in colon cancer. *Research Journal of Pharmacy and Technology*, *12*(8), 3672-3678..

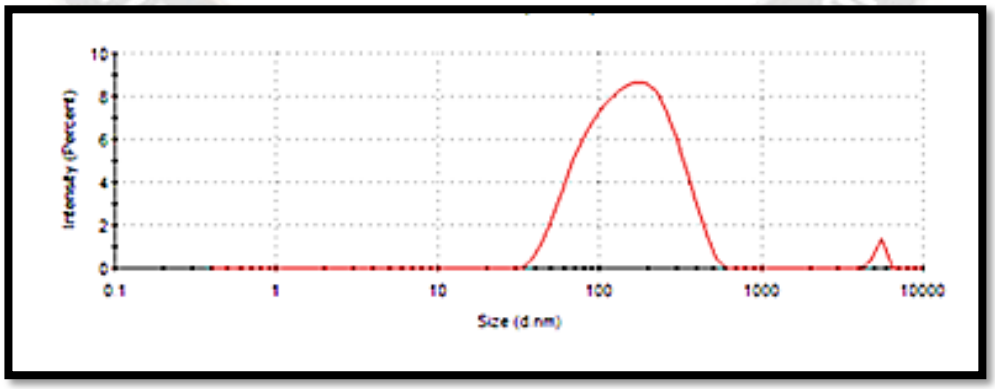

Figure 1. PSA image of MENPs

International Journal on Recent and Innovation Trends in Computing and Communication
ISSN: 2321-8169 Volume: 12 Issue: 2
Article Received: *25 November 2023* ***Revised:*** *12 December 2023* ***Accepted:*** *30 January 2024*

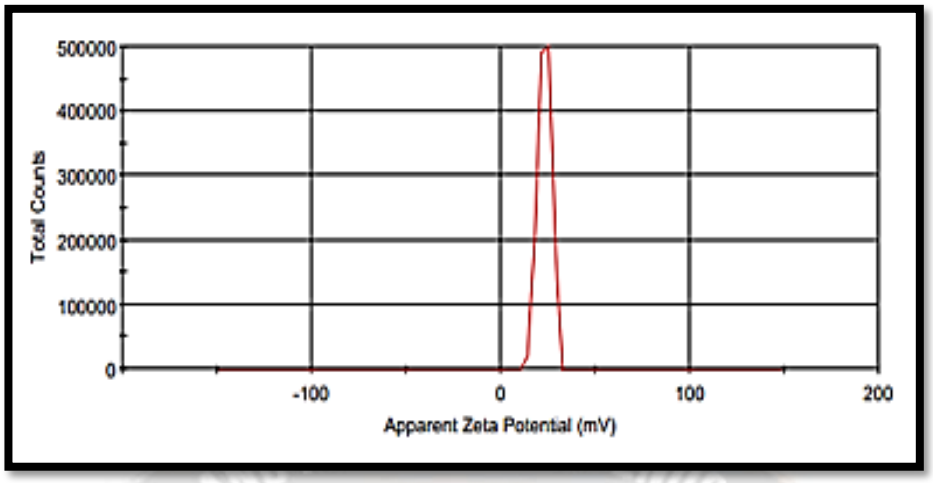

Figure 2. Zeta potential of MENPs

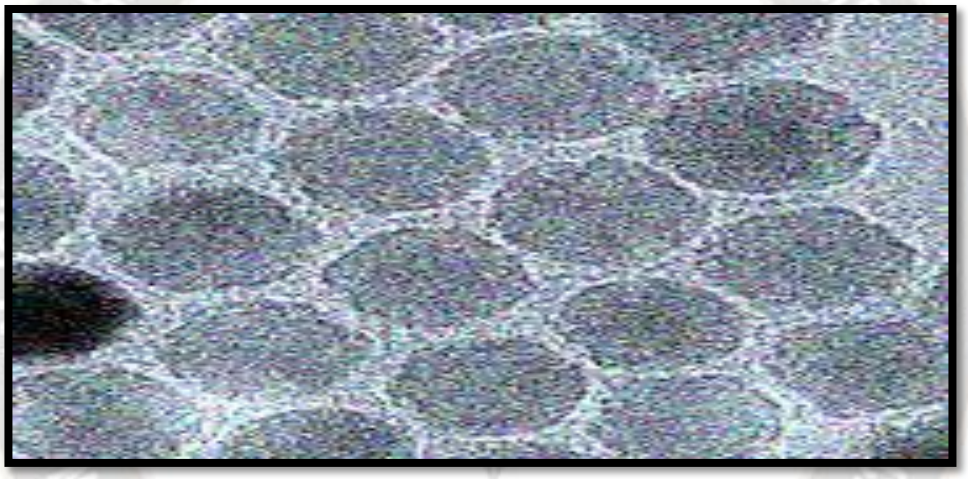

Figure 3: TEM image of MENPs

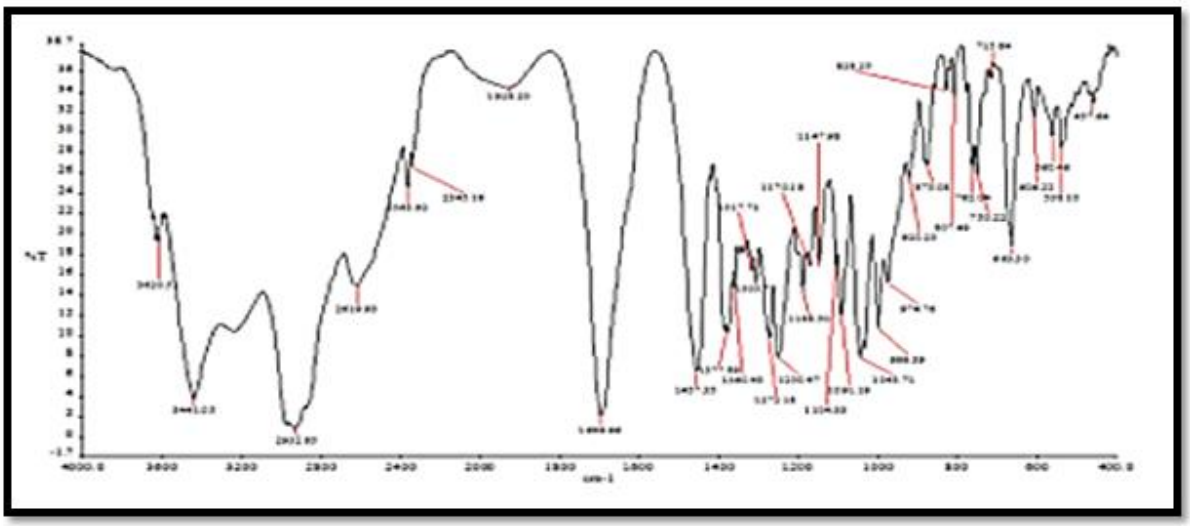

Figure 4. The FTIR spectra of MENPs

International Journal on Recent and Innovation Trends in Computing and Communication
ISSN: 2321-8169 Volume: 12 Issue: 2
Article Received: *25 November 2023* ***Revised:*** *12 December 2023* ***Accepted:*** *30 January 2024*

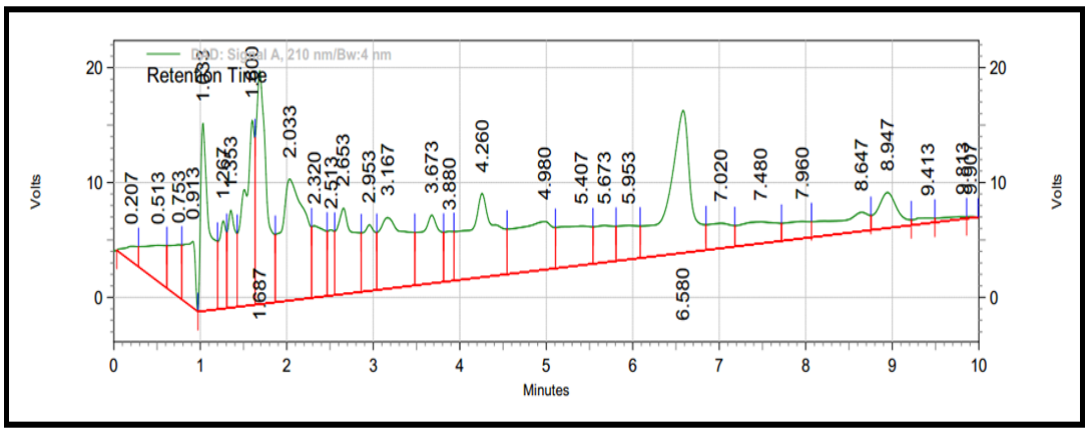

Figure 5. HPLC Chromatogram for supernatant

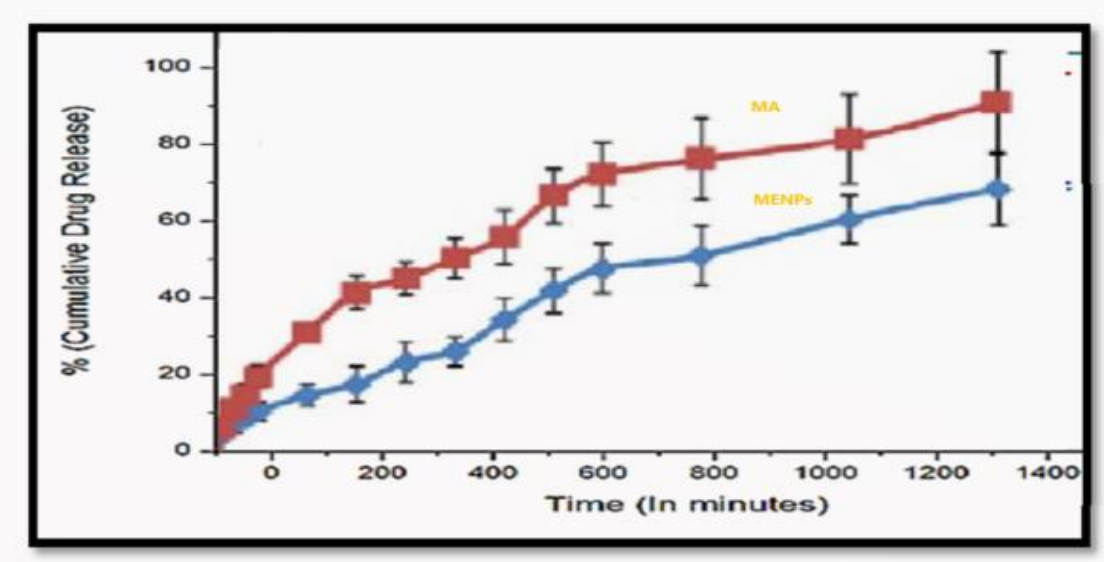

Figure 6. In-vitro release study

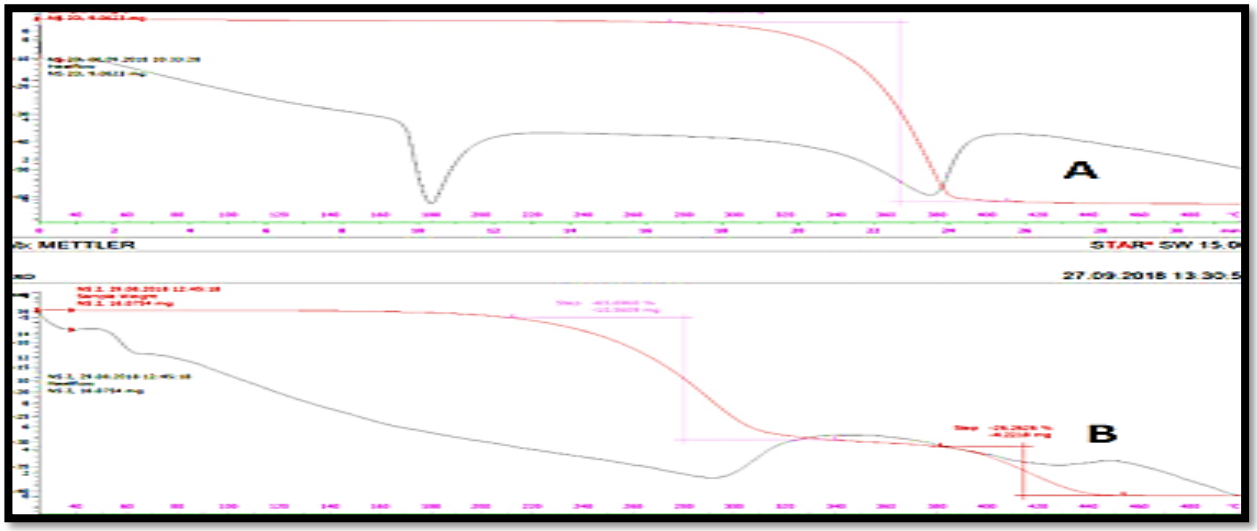

Figure 7. Differential Thermal Analysis (A) Blank Eudragit Nanoparticles (B) Drug Loaded Eudragit Nanoparticles

International Journal on Recent and Innovation Trends in Computing and Communication
ISSN: 2321-8169 Volume: 12 Issue: 2
Article Received: *25 November 2023* ***Revised:*** *12 December 2023* ***Accepted:*** *30 January 2024*

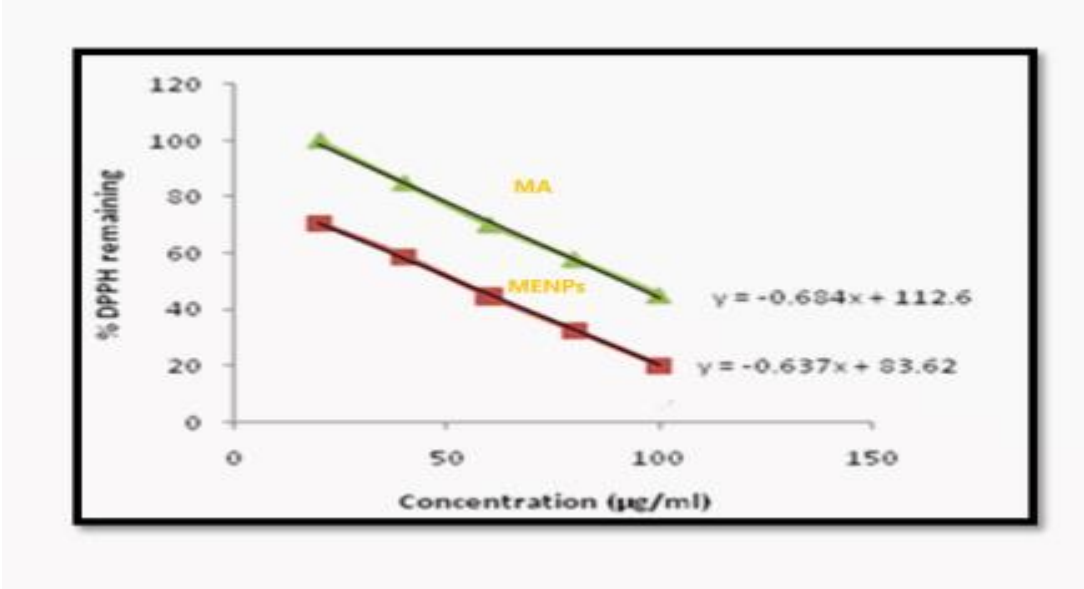

Figure 8. Antioxidant activity of MA, and MENPs

Table 1: IC50 values of MENPs along with standard drug moronic acid

Sample code	**A-549**		**MCF-7**		**Hela**	
	IC50	**pIC50**	**IC50**	**pIC50**	**IC50**	**pIC50**
MA	26.30	-1.452732	25.52	-1.4503	29.12	-1.50187
MENPs	4.3	-0.643249	3.9	-0.58106	4.1	-0.618455